

PVC-g-PSSA 가지형 공중합체를 이용한 다공성 TiO₂ 박막의 합성 및 염료감응 태양전지 응용

변수진·서진아·지원석·설용건·김종학[†]

연세대학교 화공생명공학과
(2011년 4월 27일 접수, 2011년 6월 24일 수정, 2011년 6월 24일 채택)

Synthesis of Porous TiO₂ Thin Films Using PVC-g-PSSA Graft Copolymer and Their Use in Dye-sensitized Solar Cells

Su Jin Byun, Jin Ah Seo, Won Seok Chi, Yong Gun Shul, and Jong Hak Kim[†]

Department of Chemical and Biomolecular Engineering, Yonsei University, 262 Seongsanno, Seodaemun-gu, Seoul 120-749, Korea

(Received April 27, 2011, Revised June 24, 2011, Accepted June 24, 2011)

요약: 원자전달 라디칼 중합(ATRP)에 의해 poly(vinyl chloride) (PVC) 주사슬과 poly(styrene sulfonic acid) (PSSA) 곁사슬로 되어있는 양쪽성 PVC-g-PSSA 가지형 공중합체를 합성하였다. PVC-g-PSSA 가지형 공중합체 고분자를 템플레이트로 사용하고 졸겔법을 적용하여, 결정성 아타네제상의 미세기공 이산화티타늄 필름을 제조하였다. TiO₂ 전구체인 TTIP를 친수성인 PSSA 영역과 선택적으로 작용시켜 TiO₂ 메조기공 필름을 성장하였으며, 이를 주사전자 현미경(SEM)과 엑스레이회절(XRD)분석을 통해 분석하였다. 스핀코팅 횟수와 P25 도입에 따른 염료감응 태양전지 성능을 체계적으로 분석하였다. 그 결과 준고체 고분자 전해질을 이용하였을 때, 100 mW/cm² 조건에서 에너지 변환 효율이 2.7%에 이르렀다.

Abstract: An amphiphilic graft copolymer comprising a poly(vinyl chloride) (PVC) backbone and poly(styrene sulfonic acid) (PSSA) side chains (PVC-g-PSSA) was synthesized via atom transfer radical polymerization (ATRP). Mesoporous titanium dioxide (TiO₂) films with crystalline anatase phase were synthesized via a sol-gel process by templating PVC-g-PSSA graft copolymer. Titanium isopropoxide (TTIP), a TiO₂ precursor was selectively incorporated into the hydrophilic PSSA domains of the graft copolymer and grew to form mesoporous TiO₂ films, as confirmed by scanning electron microscopy (SEM) and X-ray diffraction (XRD) analysis. The performances of dye-sensitized solar cell (DSSC) were systematically investigated by varying spin coating times and the amounts of P25 nanoparticles. The energy conversion efficiency reached up to 2.7% at 100 mW/cm² upon using quasi-solid-state polymer electrolyte.

Keywords: dye-sensitized solar cell (DSSC), sol-gel, atom transfer radical polymerization (ATRP), titanium dioxide (TiO₂), graft copolymer

1. Introduction

Polymer electrolytes have been intensively utilized in various applications such as lithium batteries [1], electrochromic devices [2], polymer electrolyte membrane fuel cells [3,4], facilitated transport membranes [5]. Recently, polymer electrolytes were also investigated as

a solid electrolyte in dye-sensitized solar cells (DSSC) [6-8]. It is because the use of liquid electrolytes might not be practical for long-term operation due to problems such as electrolyte leakage or evaporation. Thus, many research groups have been searching for alternatives to replace the liquid electrolytes, such as solid hole conductors [9], ionic liquids [10,11], gel electrolytes [12,13], quasi-solid [14,15] and solid polymer electrolytes [16,17].

[†]주저자(e-mail: jonghak@yonsei.ac.kr)

DSSCs were first reported by the Gratzel group in 1991 [18], after which they have received much attention due to global warming and the demand for cheap sources of renewable energy. In particular, DSSCs are more attractive than conventional Si-based p-n junction solar cells in terms of great design opportunities, light weight, flexibility and a low cost. DSSCs consist of a sensitizing dye, transparent conducting substrates (F-doped tin oxide), nanometer sized TiO₂ film, iodide electrolyte, and Pt-coated counter electrode. When a dye molecule absorbs light, it excites electrons on the highest occupied molecular orbital to the lowest unoccupied molecular orbital. The excited dye molecule injects an electron into the conducting band of the TiO₂ film. Preparation of mesoporous TiO₂ films with high crystallization and large surface area is of importance for enhancing the efficiency of DSSC. Thus, much prior research has focused on the development of well-organized TiO₂ films in order to an energy conversion efficiency.

A sol-gel method has many advantages such as an easy deposition on complex shaped substrates, easy control of morphology and simple equipment [19]. The preparation of sol-gel derived nanocrystals has been much investigated due to the versatility and potential for mass production [20]. In this study, we introduced a sol-gel process to synthesize mesoporous TiO₂ thin films templated by a graft copolymer, which is more attractive than a block copolymer due to its low cost and easy of synthesis. An amphiphilic graft copolymer, i.e. poly(vinyl chloride)-graft-poly(styrene sulfonic acid) (PVC-g-PSSA), consisting of PVC backbone and POEM side chains was synthesized via atom transfer radical polymerization (ATRP). The graft copolymer templated TiO₂ films have been characterized using scanning electron microscopy (SEM) and X-ray diffraction (XRD), and their efficiencies in DSSC employing quasi-solid-state polymer electrolytes are reported.

2. Experimental

2.1. Material

Poly(vinyl chloride) (PVC, $M_n = 55,000$ g/mol, $M_w = 97,000$ g/mol), 4-styrene sulfonic acid (SSA), copper(I) chloride (CuCl), 1,1,4,7,10,10-hexamethyl triethylene tetramine (HMTETA), titanium tetrakisopropoxide (TTIP, 97%), hydrochloric acid (HCl, 37%) and 1-methy-2-pyrrolidinone (NMP) were purchased from Aldrich. Methanol and dimethyl sulfoxide (DMSO) were purchased from J. T. Baker. All solvent and chemicals were reagent grade and used as received.

2.2. Synthesis of PVC-g-PSSA Graft Copolymer

PVC-g-PSSA graft copolymer was synthesized via ATRP, according to a previously reported method [21]. In brief, two grams of PVC was dissolved in 18 mL NMP in a round flask at 70°C. Separately, 14 g of SSA was dissolved in 18 mL DMSO at 70°C and added to the PVC solution. After producing homogeneous solution, 0.04 g of CuCl and 0.1 mL of HMTETA were added and the reaction flask was sealed with a rubber septum. After N₂ purging for 30 min, the reaction vessel was immersed in an oil bath at 90°C. The reaction was allowed to proceed for 24 h. After passing the solution through a column with activated Al₂O₃ to remove the catalyst, it was precipitated into methanol. The polymer was purified by redissolving in DMSO and reprecipitating in methanol. Finally, the graft copolymer was completely dried in a vacuum oven overnight at room temperature.

2.3. Preparation of Mesoporous TiO₂ Films

First, 0.9 g of PVC-g-PSSA was dissolved in 3 mL of DMSO and stirred for 24 h to ensure a clear solution. Separately, 5 mL of TTIP was slowly dropped in 2.5 mL of a HCl aqueous solution with vigorous stirring, followed by adding 2.5 mL of DI-water. After aging for 15 min, 2 mL of the TTIP sol was added to 3 mL of the PVC-g-PSSA polymer solution. The sol was aged under a mild stirring condition at room temperature for 3 h and then spin-coated on the

FTO glass with different coating times, i.e. 2, 4 and 6 times at 1,500 rpm for 20 seconds, named as No. 1, 2 and 3. For the sample of No. 4, P25 (Degussa) nanoparticles of 0.5 g were added to the sol. The resultant sols were well dispersed using speed control Type 37,600 mixer for several seconds. Then, the viscous sols were cast on the FTO-glass using a doctor blading method.

2.4. Fabrication of DSSCs

DSSCs with an active area of 0.4 cm² were constructed by drop-casting of electrolyte solution onto the photoelectrode and covering with the counter electrode, according to previous reported procedure [22-24]. In order to prepare photoelectrodes, conductive FTO glasses were first coated by titanium diisopropoxide bis (acetylacetonate) 75 wt% solution in 2-propanol. After drying at 50°C for 30 min, the photoelectrodes were heated at 450°C for 30 min, followed by cooling to room temperature for 8 hours. The Pt counter electrodes were prepared by spin coating hydrogen hexachloroplatinate (IV) hexahydrate solution (H₂PtCl₆) onto the FTO glasses. Then, the counter electrodes were heated to 450°C for 30 min. The photo electrode was spin coated with the solution at 1,500 rpm for 20 sec. The photo electrode was sintered at 450°C for 30 min to obtain mesoporous TiO₂ film. After being sintered, the TiO₂ electrodes were immersed into a solution of an amphiphilic dye (Ruthenium 35-bisTBA, N719, Solaronix SA) in absolute ethanol for 2 hours at 50°C. After drying the dye-adsorbed photoelectrodes at room temperature, polymer electrolyte solutions were cast onto the dye-adsorbed TiO₂ electrodes. A quasi-solid polymer electrolyte solution was prepared by dissolving fumed silica nanoparticles (SiO₂), PEGDME, MPPI, and I₂ in acetonitrile [23]. The mole ratio of ether oxygen to iodide salt was fixed at 20, and the iodine content was fixed at 10 wt% with respect to the salt. The cells were placed in a vacuum oven for a day to permit complete evaporation of solvent and were then sealed with an epoxy resin.

Photoelectrochemical performance characteristics, in-

cluding short-circuit current (J_{sc} , mA/cm²), open-circuit voltage (V_{oc} , V), fill factor (ff), and overall energy conversion efficiency (η) were measured using a Keithley Model 2,400 and a 1000 W xenon lamp (Oriol, 91193). The light was homogeneous over an 8 × 8 in² area, and its intensity was calibrated with a Si solar cell (Fraunhofer Institute for Solar Energy System, Mono-Si+KG filter, Certificate No. C-ISE269) for a sun light intensity of 1 (100 mW/cm²). This calibration was double-checked with a NREL-calibrated Si solar cell (PV Measurements Inc.). Photoelectrochemical performance was calculated using the following equations:

$$FF = \frac{V_{max} \cdot J_{max}}{V_{oc} \cdot J_{sc}} \quad (1)$$

$$\eta (\%) = \frac{V_{max} \cdot J_{max}}{P_{in}} \times 100 = \frac{V_{oc} \cdot J_{sc} \cdot ff}{P_{in}} \times 100 \quad (2)$$

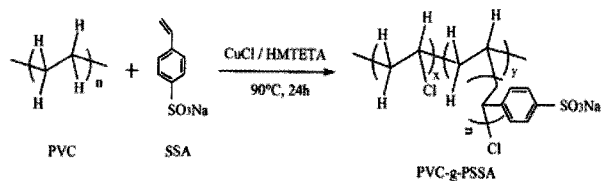
where J_{sc} is the short-circuit current density (mA/cm²), V_{oc} is the open-circuit voltage (V), P_{in} is the incident light power, and J_{max} (mA/cm²) and V_{max} (V) are the current density and voltage in the J - V curve, respectively, at the point of maximum power output.

2.5. Characterization

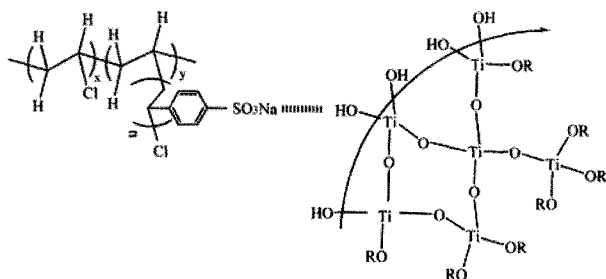
FT-IR spectra of samples were performed on Perkin Elmer spectrum 100, between frequency 4,000~600 cm⁻¹ using an ATR. FE-SEM image was obtained to observe the morphology of TiO₂ film from Bruker D8 DISCOVER (Carl Zeiss, Germany). UV-visible spectroscopy was measured with spectrophotometer (Hewlett Packard) in the range of 300 to 800 nm. The XRD experiment was performed on a Rigaku 18 kW rotating anode X-ray generator with Cu-K α radiation operated at 40 kV and 300 mA.

2.6. Measurement of Dye Adsorption

First, the N719 dye-sensitized TiO₂ photoelectrode was dipped into 10.0 mL of a 10⁻² M solution of NaOH in ethanol-H₂O (1 : 1). The mixture was stirred until complete desorption of the dye into the liquid



Scheme 1. Synthesis of PVC-g-PSSA graft copolymer by ATRP.



Scheme 2. Interaction between PVC-g-PSSA graft copolymer and TiO₂ sol-gel solution.

occurred. The volume of the NaOH solution containing the fully desorbed dye was then carefully measured by UV-visible spectroscopy. The amounts of the NaOH solutions were recorded, and the absorption value at 515 nm (as a function of wavelength) was used to calculate the number of adsorbed N719 dye molecules according to the Beer-Lambert law, $A = \epsilon lc$, where A is the absorbance of the UV-visible spectra at 515 nm, $\epsilon = 14,100/\text{M cm}$ is the molar extinction coefficient of the dye at 515 nm, l is the path length of the light beam, and c is the dye concentration [23].

3. Results and Discussion

PVC-g-PSSA graft copolymer was synthesized via one-step ATRP, as illustrated in Scheme 1. This copolymer was combined with a TiO₂ precursor, i.e. TTIP to produce graft copolymer/TiO₂ hybrid via a sol-gel process. Because of hydrophilicity, TTIP is preferentially incorporated into the hydrophilic PSSA domains of the graft copolymer and grows to form TiO₂ nanoparticles [25]. Upon calcination, the hydrophobic PVC domains were completely burn out to gen-

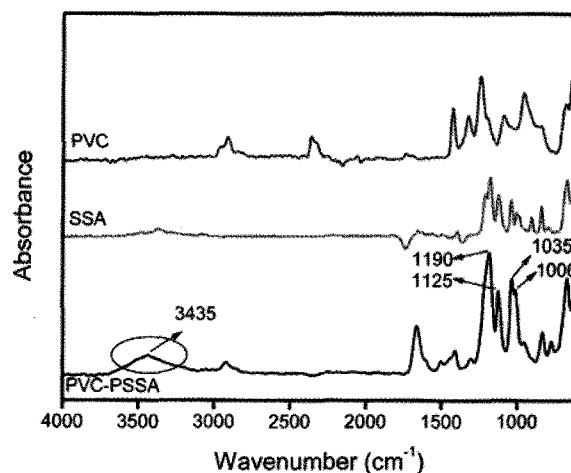


Fig. 1. FT-IR spectra of pristine PVC, SSA and PVC-g-PSSA graft copolymer.

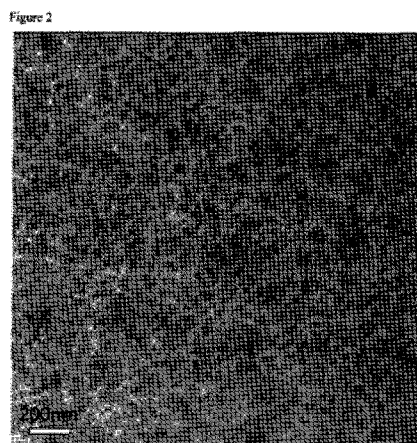


Fig. 2. TEM image of PVC-g-PSSA graft copolymer.

erate pores whereas PSSA/TTIP produced the TiO₂ matrix, as shown in Scheme 2.

Fig. 1 shows the FT-IR spectra of pristine PVC and its graft copolymer with PSSA. Compared to the pristine PVC, the PVC-g-PSSA graft copolymer exhibited the strong absorption bands at 1,190, 1,125, 1,035 and 1,006 cm⁻¹. These bands result from the stretching vibrations of phenyl rings substituted with sulfonate groups and sulfonate anions attached to phenyl ring [26]. The broad absorption band at around 3,435 cm⁻¹ is attributed to the water bounded to ionic groups of the graft copolymer.

TEM analysis was carried out to characterize the

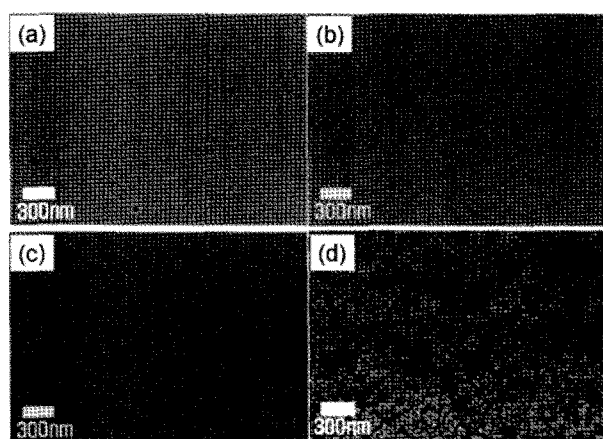


Fig. 3. SEM images of mesoporous TiO₂ films prepared with different compositions of PVC-g-PSSA and TTIP; (a) No 1, (b) No 2, (c) No 3 and (d) No 4.

morphology of PVC-g-PSSA graft copolymer, as shown in Fig. 2. The large difference of electron densities between the PVC main chains and the PSSA side chains produces amphiphilic property and thus provides clear image contrast between two domains [17]. Dark regions represent the hydrophobic domains of PVC main chains whereas lighter regions do the PSSA side chains. The PVC-g-PSSA graft copolymer self-assembled into the hydrophobic domains of PVC main chains with the hydrophilic domains of PSSA brush layer, resulting from chemical dissimilarity between the two polymer segments.

SEM analysis was used to characterize the morphology of PVC-g-PSSA/TTIP films after calcination at 450°C. A TiO₂ precursor, TTIP is selectively incorporated into the hydrophilic PSSA domains of the graft copolymer and grows to form TiO₂ nanoparticles, as illustrated in Scheme 2. The SEM images of Fig. 3 shows randomly distributed pores at film surface and their size is approximately 30 nm. Fig. 3(a)~(c) shows the effect of coating time on the TiO₂ morphology. Generally, the number of pores increased with an increase in coating time of sol-gel solution. Upon the introduction of P25 powder (Fig. 3d), spherical particles grew up uniformly and covered the whole surface of TiO₂ film.

The structural patterns of PVC-g-PSSA graft copoly-

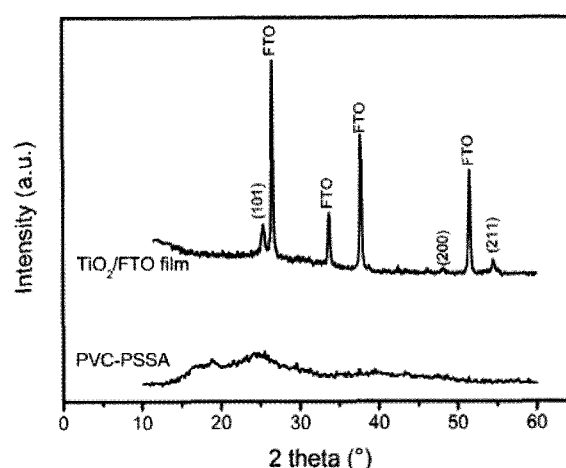


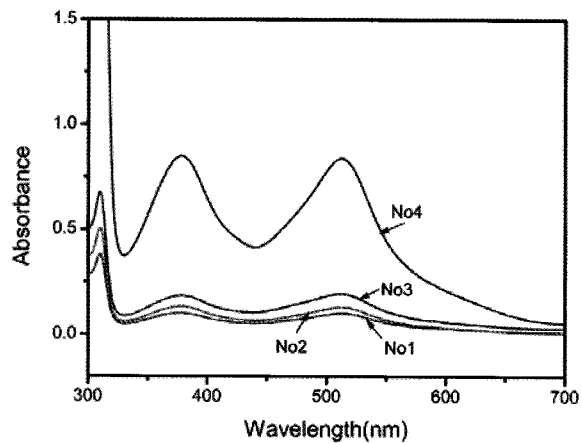
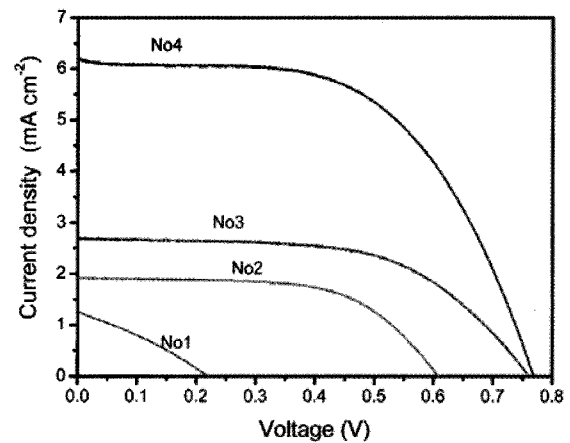
Fig. 4. XRD patterns of PVC-g-PSSA graft copolymer and mesoporous TiO₂ film (No 3).

mer and the crystallized mesoporous TiO₂ thin film templated by PVC-g-PSSA were investigated using XRD analysis, as presented in Fig. 4. Neat PVC-g-PSSA graft copolymer exhibited some weak peaks at 16.7°, 18.9°, and 24.6°, indicating its amorphous state. The mesoporous TiO₂ thin film showed several crystalline sharp peaks at 25.3°, 48.2° and 54.5°, which are attributed to (101), (200), and (211) planes, respectively, of the anatase TiO₂ phase [27,28]. It represents that the structural changes and phase transformation of TiO₂ to crystalline anatase occurred at around 450°C. The rest of the strong peaks arose from the FTO glass. There was no amorphous peak from graft copolymer in the mesoporous TiO₂ thin film, indicating complete calcination of the organic template.

The efficiency of DSSC strongly depends on the amount of dye adsorption, which is related, in turn, to the structure of the TiO₂ film. The dye adsorption of the mesoporous TiO₂ films were measured by adsorption-desorption experiments. Fig. 5 shows the UV-visible absorption spectra for dye adsorption onto the TiO₂ films and their results were summarized in Table 1. The strong absorption at around 515 nm is attributed to N719 dye molecules. The amount of dye adsorption was different depending on the kind of TiO₂ films and affected by the number of spin coating times and the presence of P25. The amount of dye adsorption was

Table 1. Dye adsorption amounts and performance parameters of DSSC fabricated with different types of TiO₂ photoelectrodes at 100 mW/cm²

Sample	Thickness (μm)	Dye adsorbed (nmol/cm ²)	V _{oc} (V)	J _{sc} (mA/cm ²)	FF	η (%)
No 1	0.7	14.2	0.22	1.27	0.30	0.08
No 2	1.5	18.3	0.61	1.92	0.58	0.68
No 3	3.8	27.3	0.76	2.69	0.56	1.15
No 4	12.0	118	0.77	6.21	0.55	2.64

**Fig. 5.** UV-visible spectra for the dye adsorption in mesoporous TiO₂ films prepared with different compositions of PVC-g-PSSA and TTIP.**Fig. 6.** Current-voltage characteristics of DSSC fabricated with different types of TiO₂ photoelectrodes at 100 mW/cm².

arranged in the following order: No 1 < No 2 < No 3 < No 4.

In order to examine the photoelectrochemical performance, the photocurrent density-voltage characteristics of DSSC were measured at 100 mW/cm² as shown in Fig. 6 and summarized in Table 1. The energy conversion efficiency continuously increased with the thickness of TiO₂ film, which was also related to the amount of dye adsorption. The performance of DSSCs was arranged in the following order: No 1 < No 2 < No 3 < No 4, which is consistent with the sequence of amount of dye adsorption. The DSSC of No 4 showed improved the J_{sc} and V_{oc} values and a better performance of 2.64% at 100 mW/cm². It results from the large amounts of dye adsorption due to larger thickness of mesoporous TiO₂ film.

4. Conclusions

Amphiphilic PVC-g-PSSA graft copolymer was synthesized via ATRP technique using PVC backbone as a macroinitiator and used as a template for the preparation of mesoporous titanium dioxide (TiO₂) film for DSSC. Synthesis of microphase-separated PVC-g-PSSA graft copolymer was successful via a grafting-from method using ATRP. The graft copolymer was molecularly combined with a TiO₂ precursor, TTIP to produce graft copolymer/TiO₂ nanocomposite membranes via a sol-gel process. A hydrophilic TTIP was selectively confined into the hydrophilic PSSA domains of the graft copolymer and grew to form TiO₂ nanoparticles. The porosity of mesoporous TiO₂ film and the effect of spin coating times were investigated. As a result, the DSSC of No 4 with large spin coating time and the presence of P25 nanoparticles showed the highest

energy conversion efficiency of 2.64% at 100 mW/cm².

Acknowledgement

This work was supported by the Ministry of Knowledge Economy through the Human Resources Development of the Korea Institute of Energy Technology Evaluation and Planning (KETEP) (20104010100500) and New & Renewable Energy R&D program (2009T100100606). This work was also supported by the Ministry of Knowledge Economy (MKE) and Korea Institute for Advancement in Technology (KIAT) through the Workforce Development Program in Strategic Technology.

References

1. N. Yoshimoto, O. Shimamura, T. Nishimura, M. Egashira, M. Nichioka, and M. Morita, "A novel polymeric electrolyte based on a copolymer containing self-assembled stearyl moiety for lithium-ion batteries", *Electrochem. Commun.*, **11**, 481 (2009).
2. J. Lee, Y. Kim, and E. Kim, "Electrochromic Property of a Conductive Polymer Film Fabricated with Vapor Phase Polymerization", *Membrane Journal*, **20**, 8 (2010).
3. B. L. Langsdorf, J. Sultan, and P. G. Pickup, "Partitioning and polymerization of pyrrole into perfluorosulfonate (Nafion) membranes under neutral conditions", *J. Phys. Chem. B*, **107**, 8412 (2003).
4. H. Ko, J. Park, J. Choi, S. U. Kim, H. J. Kim, and Y. T. Hong, "Double-layered polymer electrolyte membrane based on sulfonated poly(aryl ether sulfone)s for direct methanol fuel cells", *Membrane Journal*, **19**, 291 (2009).
5. J. H. Kim, B. R. Min, J. Won, S. H. Joo, H. S. Kim, and Y. S. Kang, "Role of polymer matrix in polymer/silver complexes for structure, interactions, and facilitated olefin transport", *Macromolecules*, **36**, 6183 (2003).
6. T. Stergiopoulos, I. M. Arabatzis, G. Katsaros, and P. Falaras, "Binary polyethylene oxide/titania solid-state redox electrolyte for highly efficient nanocrystalline TiO₂ photoelectrochemical cells", *Nano Lett.*, **2**, 1259 (2002).
7. M.-J. Choi, C.-H. Shin, T. Kang, J.-K. Koo, and N. Cho, "A study on the organic/inorganic composite electrolyte membranes for dye sensitized solar cell", *Membrane Journal*, **18**, 345 (2008).
8. M. Wang, X. Xiao, X. Zhou, X. Li, and Y. Lin, "Investigation of PEO-imidazole ionic liquid oligomer electrolytes for dye-sensitized solar cells", *Sol. Energy Mater. Sol. Cells*, **91**, 785 (2007).
9. J. E. Kroeze, N. Hirata, L. Schmidt-Mende, C. Orizu, S. D. Ogier, K. Carr, M. Gratzel, and J. R. Durrant, "Parameters Influencing Charge Separation in Solid-State Dye-Sensitized Solar Cells Using Novel Hole Conductors", *Adv. Funct. Mater.*, **16**, 1832 (2006).
10. M. Wang, X. Xiao, X. Zhou, X. Li, and Y. Lin, "Investigation of PEO-imidazole ionic liquid oligomer electrolytes for dye-sensitized solar cells", *Sol. Energy Mater. Sol. Cells*, **91**, 785 (2007).
11. N. Yamanaka, R. Kawano, W. Kubo, N. Masaki, T. Kitamura, Y. Wada, M. Watanabe, and S. Yanagida, "Dye-Sensitized TiO₂ Solar Cells Using Imidazolium-Type Ionic Liquid Crystal Systems as Effective Electrolytes", *J. Phys. Chem. B*, **111**, 4763 (2007).
12. P. Wang, S. M. Zakeeruddin, J. E. Moser, M. K. Nazeeruddin, T. Sekiguchi, and M. Grätzel, "A stable quasi-solid-state dye-sensitized solar cell with an amphiphilic ruthenium sensitizer and polymer gel electrolyte", *Nature Mater.*, **2**, 402 (2003).
13. W. Kubo, K. Murakoshi, T. Kitamura, S. Yoshida, M. Haruki, K. Hanabusa, H. Shirai, Y. Wada, and S. Yanagida, "Quasi-solid-state dye-sensitized TiO₂ solar cells: effective charge transport in mesoporous space filled with gel electrolytes containing iodide and iodine", *J. Phys. Chem. B*, **105**, 12809 (2001).
14. G. D. Sharma, P. Suresh, M. S. Roy, and J. A. Mikroyannidis, "Effect of surface modification of TiO₂ on the photovoltaic performance of the quasi

- solid state dye sensitized solar cells using a benzo-thiadiazole-based dye”, *J. Power Sources*, **195**, 3011 (2010).
15. J. A. Mikroyannidis, M. M. Stylianakis, M. S. Roy, P. Suresh, and G. D. Sharma, “Synthesis, photophysics of two new perylene bisimides and their photovoltaic performances in quasi solid state dye sensitized solar cells”, *J. Power Sources*, **194**, 1171 (2009).
 16. I. C. Flores, J. N. Freitas, C. Longo, M. A. Paoli, H. Winnischofer, and A. F. Nogueira, “Dye-sensitized solar cells based on TiO₂ nanotubes and a solid-state electrolyte”, *J. Photochem. Photobio. A: Chem.*, **189**, 153 (2007).
 17. T. Kang, C. H. Shin, M.-J. Choi, J. K. Koo, and N. Cho, “A study on the ionic conducting characteristics of electrolyte membranes containing KI and I₂ for dye sensitized solar cell”, *Membrane Journal*, **20**, 21 (2010).
 18. B. O'Reagan and M. Grätzel, “A low-cost, high-efficiency solar cell based on dye-sensitized colloidal TiO₂ films”, *Nature*, **353**, 737 (1991).
 19. Y. Lee, J. Chae, and M. Kang, “Comparison of the photovoltaic efficiency on DSSC for nanometer sized TiO₂ using a conventional sol-gel and solvothermal methods”, *J. Ind. Eng. Chem.*, **16**, 609 (2010).
 20. X. Hu, G. Li, and J. C. Yu, “Design, Fabrication, and Modification of Nanostructured Semiconductor Materials for Environmental and Energy Applications”, *Langmuir*, **26**, 3031 (2010).
 21. J. K. Choi, Y. W. Kim, J. H. Koh, and J. H. Kim, “Proton Conducting Membranes Based on Poly(vinyl chloride) Graft Copolymer Electrolytes”, *Polym. Adv. Technol.*, **19**, 915 (2008).
 22. S. H. Ahn, J. H. Koh, J. A. Seo, and J. H. Kim, “Structure control of organized mesoporous TiO₂ films templated by graft copolymers for dye-sensitized solar cells”, *Chem. Commun.*, **46**, 1935 (2010).
 23. J. T. Park, D. K. Roh, R. Patel, E. Kim, D. Y. Ryu, and J. H. Kim, “Preparation of TiO₂ Spheres with Hierarchical Pores via Grafting Polymerization and Sol-gel Process for Dye-Sensitized Solar Cells”, *J. Mater. Chem.*, **20**, 8521 (2010).
 24. J. K. Koh, J. Kim, B. Kim, J. H. Kim, and E. Kim, “Highly Efficient Iodine-Free Dye-Sensitized Solar Cells with Solid-State Synthesis of Conducting Polymers”, *Adv. Mater.*, **23**, 1641 (2011).
 25. N. Perkass, M. Shuster, G. Amirian, Y. Koltypin, and A. Gedanken, “Sonochemical immobilization of silver nanoparticles on porous polypropylene”, *J. Polym. Sci. A: Polym. Chem.*, **46**, 1719 (2008).
 26. A. Mokrini and J. L. Acosta, “Studies of sulfonated block copolymer and its blends”, *Polymer*, **42**, 9 (2001).
 27. P. C. A. Alberius, K. L. Frindell, R. C. Hayward, E. J. Kramer, G. D. Stucky, and B. F. Chmelka, “General predictive syntheses of cubic, hexagonal, and lamellar silica and titania mesostructured thin films”, *Chem. Mater.*, **14**, 3284, (2002).
 28. P. Falaras, T. Stergiopoulos, and D. S. Tsoukleris, “Enhanced efficiency in solid-state dye-sensitized solar cells based on fractal nanostructured TiO₂ thin films”, *Small*, **4**, 770 (2008).